

High Altitude Balloon
Phys 450
April 11, 2008

Andrew Ringeri
Evan Hau
Robbie Edwards
Ryan Hairsine

Abstract

A high altitude helium balloon was sent up approximately 30 km into the atmosphere and tracked using GPS. The balloon was made of totex and designed to expand as the altitude increased and eventually burst at the design altitude of 30 km. After bursting, the balloon released a parachute which guided the payload safely to the ground. The purpose of the balloon was to take photographs and take atmospheric measurements. Systems to measure the pressure, temperature, and cosmic ray activity as a function of altitude were designed and constructed, however, due to weight restrictions and last minute failures, no measurements were taken. All of the instrumentation was powered by two 3.7V, 5700 mAh lithium polymer batteries and fully controlled by three PIC microchips. The balloon launch took place on March 30, 2008 near Maynooth, ON. The final landing location of the payload was deep in the Adirondacks Park. The payload was successfully tracked and recovered with all instrumentation still intact, including 865 MB worth of good quality pictures. Pictures up to 153 minutes of flight time were recorded and were used in calculating the altitude of the balloon.

Table of Contents

Purpose	1
Goals	1
Design Method	1
Payload, Parachute and Balloon	2
Payload Capsule.....	2
Balloon.....	2
Parachute.....	3
Weight.....	4
Power systems	4
Microcontroller	7
Purpose.....	7
Design	7
Challenges.....	8
Camera system	9
Sensors	10
Purpose.....	10
Temperature Sensor	10
Pressure Sensor	13
Sensors During Flight	16
Cosmic Ray Detector	17
Introduction.....	17
Detector.....	17
Power Supply	18
Signal Amplification.....	18
Testing.....	20
Tracking System	20
Cut Down Timer	23
Photos and Analysis	24
Conclusion	30
References	30
Appendices	31
Appendix A: Thermistor Current Source.....	31
Appendix B: Voltage Offset for Sensors	31
Appendix C: Design calculations of cosmic ray detector power circuit.....	33

Purpose

The purpose of this project was to construct a payload that would consist of instrumentation carried by a helium filled balloon to altitudes of approximately 30km which would take pressure, temperature and cosmic ray activity measurements during the duration of the flight. A digital camera would also be attached to the payload exterior in order to capture aerial photos of the flight. The payload would be tracked throughout the flight and, upon landing, retrieved for data analysis.

Goals

The goals of the project were as follows:

- Achieve an altitude of 30 km
- Take photographs
 - servomotor control to achieve photographs taken at various angles of depression
- Design and construction of temperature, pressure, cosmic ray activity
 - Obtain data
- Tracking of the balloon in flight
- Safe recovery of payload and instrumentation
- Design balloon within limitations
 - Power
 - Weight
 - Cost

Design Method

The design method used was an iterative process and is best illustrated in the flow chart shown below:

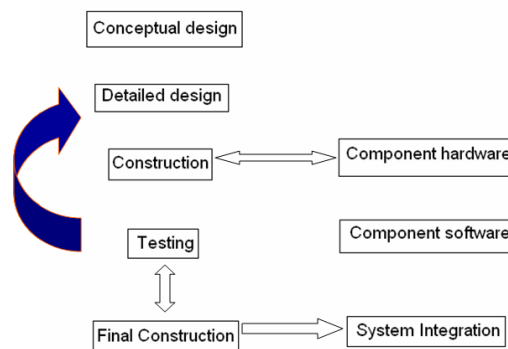


Figure 1 - High altitude balloon design methodology.

Payload, Parachute and Balloon

Payload Capsule

The main purpose of the payload capsule was to provide a means by which to carry the instrumentation, insulate the electronics and to dampen the force felt by its contents as it impacts the earth upon landing. The payload capsule was constructed out of 3/4" insulating foam with inner dimensions of 7x7x9 inches. The capsule was carried in a nylon jacket with rings fastened at each upper corner to which the parachute was connected. The jacket was necessary to ensure the parachute did not detach from the payload capsule once fully deployed. All instrumentation was contained within the capsule during flight except for the digital camera which was mounted externally as shown in Figure 2.

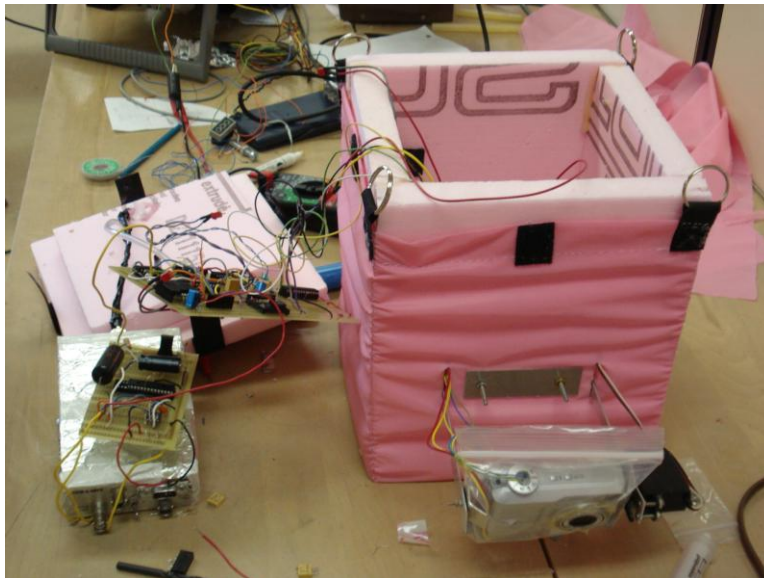


Figure 2 - Payload capsule.

Balloon

The balloon was a totex sounding balloon purchased from Kaymont Meteorological Balloons. Its specifications are shown in Table 1.

Table 1 - Balloon specifications [Kaymont Meteorological Balloons].

	KCL 1500
Average Weight (g)	1500
Neck Diameter (cm)	3
Neck Length (cm)	12
Payload (g)	1050
Recommended Free Lift (g)	1280
Nozzle Lift (g)	2330

Gross Lift (g)	3830
Diameter at release (cm)	185
Volume at release (m ³)	3.33
Diameter at burst (cm)	944

Using the relationship:

$$\frac{P_1}{P_2} = \frac{V_2}{V_1} \quad (1)$$

Where P_1 and V_1 are the pressure and volume respectively at launch altitude, and P_2 and V_2 are the pressure and volume at bursting altitude. Using balloon specification and atmospheric pressure versus altitude data it was found that the balloon would burst at an altitude of 34.2km. The balloon would be filled with helium gas (which provides the lift values as given in Table 1) from a compressed storage tank and Equation 1 was used to determine the volume transferred from the tank to the balloon using the tank's pressure gauge.

The mass that the filled balloon would be capable of lifting is given by the following equation:

$$m = \rho_{air} V_{air} - \rho_{helium} V_{helium} \quad (2)$$

Where ρ is the respective gas densities and V is the volume of lifting gas. Therefore, the maximum total weight that could be lifted by the volume of helium given by the balloon's specifications at release would be 3.83 kg.

Parachute

The purpose of the parachute was to slow the rate of decent to minimize damage on impact. The parachute was a 6 ft diameter low-porosity ripstop purchased from the Rocketman Store. The bottom of the parachute was connected to the payload capsule and the top of the parachute was connected to the balloon by a 30ft long nylon rope. The equation used to determine the rate of decent was given by:

$$V = \sqrt{\frac{8mg}{\pi\rho D^2 C_D}} \quad (3)$$

Where m is the mass of the descending payload, g is the acceleration due to gravity, ρ is the density of air, D is the diameter of the parachute and C_D is the coefficient of drag for the parachute (approximately 0.2).

The entire balloon configuration is shown in Figure 3.



Figure 3 - High altitude balloon configuration.

Weight

Power systems

For the most part of the project the specific requirements for a power system were unclear. The original design called for a single 3.7V, 5.3Ah Lithium Polymer cell to provide all the power to the balloon. Lithium Polymer (Lipo) was chosen based on a very high energy storage to mass ratio and a low response to a decrease in temperature. It is well known in the industry that lithium cells, which are used by the military, do not show a significant power drop in cold weather. Although the quantitative temperature response of Lipo batteries is unknown, they have been used in high altitude projects before. After an initial failed order from www.cheapbatterypacks.com, two identical 5700mAh cells were purchased from www.all-battery.com. They were attached to a foam mount, wired in series and tapped with a Dean's Micro Plug giving a total of 5700mAh with an operating voltage range of 8.4 – 6V. Using an average of 3.7 V per cell this amounts to an estimate of 151 848J of storage. The total weight of the batteries was 280g.

As the specific voltage and current requirements became clear, voltage regulators and DC step ups were ordered. The power requirements are given in Table 1. The power system used to meet these requirements is given in Figure 1. The circuit in Figure 2 was built to provide a step up from 8V to 48V for the bias of the detector. Separate grounds were used

to achieve the $\pm 24V$. Considerable time was spent to achieve proper operation of this circuit

Table 1: Component power consumption

Component	Voltage [V]	Current [A]	Power [W]
Microtrak 8000F/A + GPS	12	0.80 (1s / 21s) + 0.01	0.58
Camera	5	0.56	2.80
Camera Servo	5	0.4 (1s/17s)	0.18
Silicon detector	$\sim -24 + 24$	0.01	0.48
detector preamp	5	??	??
PICS	5	0.024	0.12
Op amps	$\sim -15+15$	0.018	0.54
		Total:	4.70

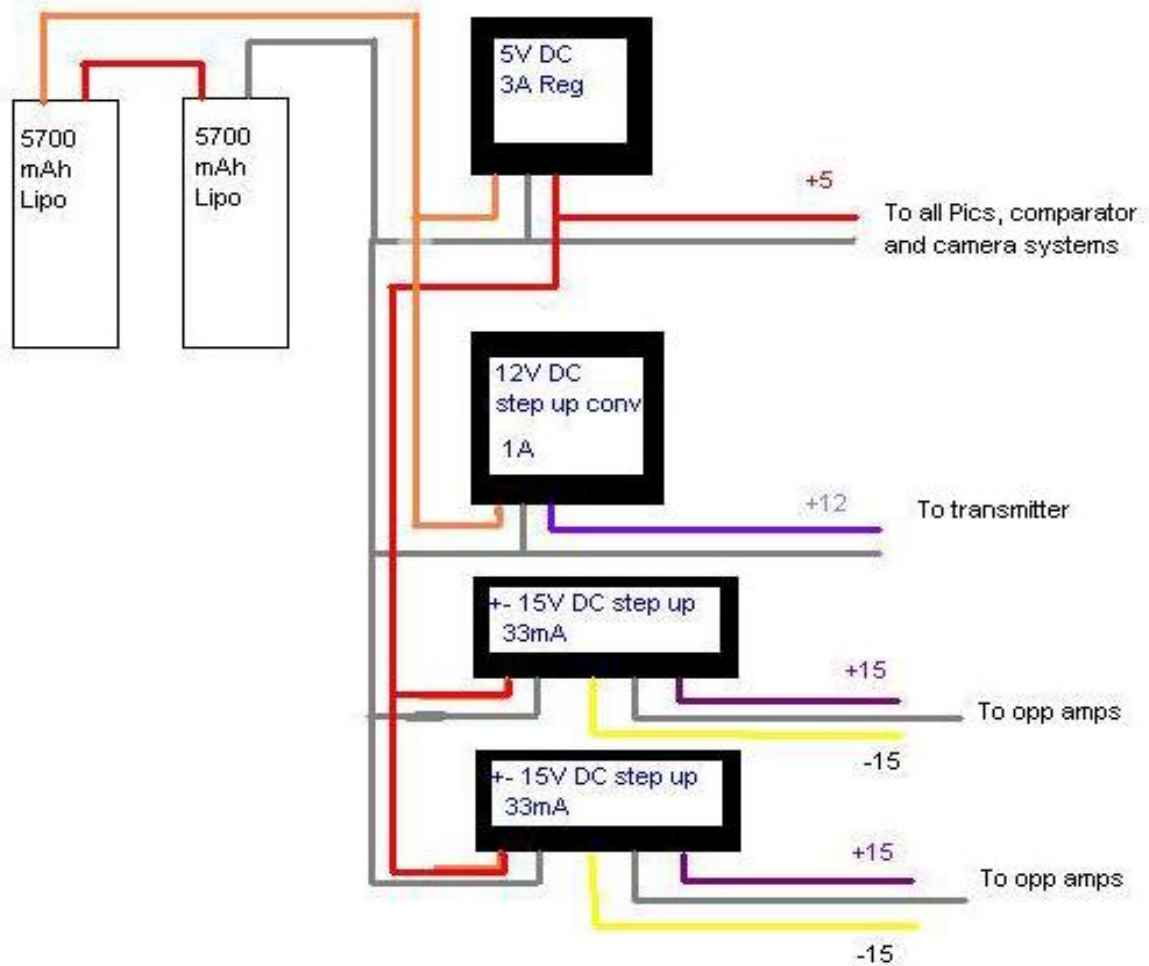


Figure 1: Regulators and step ups used to supply necessary voltages to the circuits in the payload.

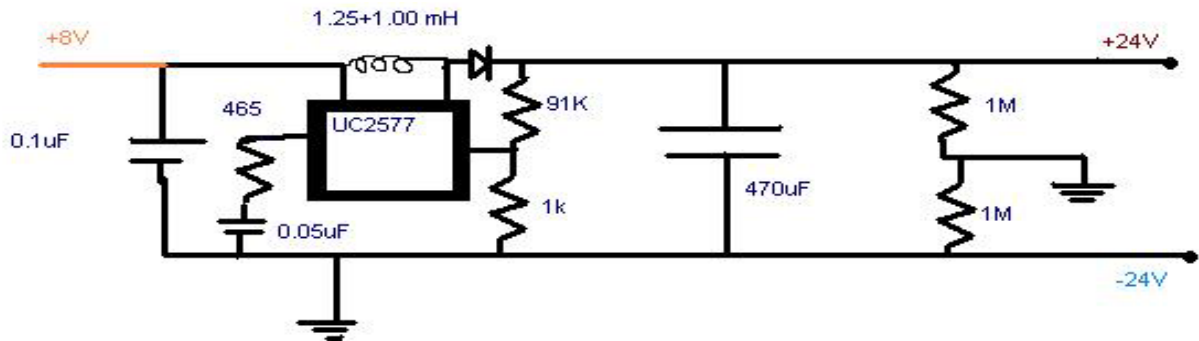


Figure 2: Step up circuit used for the detector bias.

The efficiencies of the regulators and step ups fell between 80 and 90% and varied as a function of current. With the total power consumption given in [Table 1](#) and efficiencies of the regulators it was expected that the batteries would last just over 8 hours if they

were not severely affected by the cold. The power system maintained power from the time of launch at 3:45 until far after landing at 11:45 pm in the evening (8 hours!). Note that the camera system was disabled after 153mins, the silicon detector and preamp were removed before launch and the pressure and temp op amps were disabled. On April 1st 2008 at 12:01 at night the transmitter powered back on and began transmitting packets which were received on average every 6 minutes until 12:25 noon the same day. This could be due to an increase in outdoor temperature but none the less, was entirely unexpected. The batteries were found at 1.5V below their minimum operating voltage of 3V per cell.

Microcontroller

Purpose

A microcontroller was used for the automatic data logging of instrumentation and control of the camera shutter. By using a microcontroller, the data acquisition and camera control could be customized to suite the flight of the payload.

A PIC MicroChip microcontroller was selected over a STAMP microcontroller as they retailed at \$5 per chip, as opposed to the STAMP which retailed at \$50. The cheaper microcontroller was selected so that there was no fear of shorting a \$50 device, and a greater number of devices could be implemented on the payload without exceeding the budget. The technical staff at the Physics Department also had available three 18f2620 PIC microcontrollers and a PicStart Plus programmer, which allowed the team to begin learning about microcontrollers early in the design process.

Design

Circuit

Figure 3 shows the pin diagram for the 18f2620 microcontroller. The circuit for the 18f2620 microcontroller consisted of grounding pin 8 and pin 19, 5V power supply at pin 20 and holding MCLR pin1 at 5V. The 5V regulated power supply eliminated the need for protection diodes and an electrolytic capacitor across V_{dd} and V_{ss} . Port A of the microcontroller was used as analog inputs, and Port B as the digital I/O. The internal oscillator was used and set at 8MHz and a 5V ADC reference voltage at pin 4.

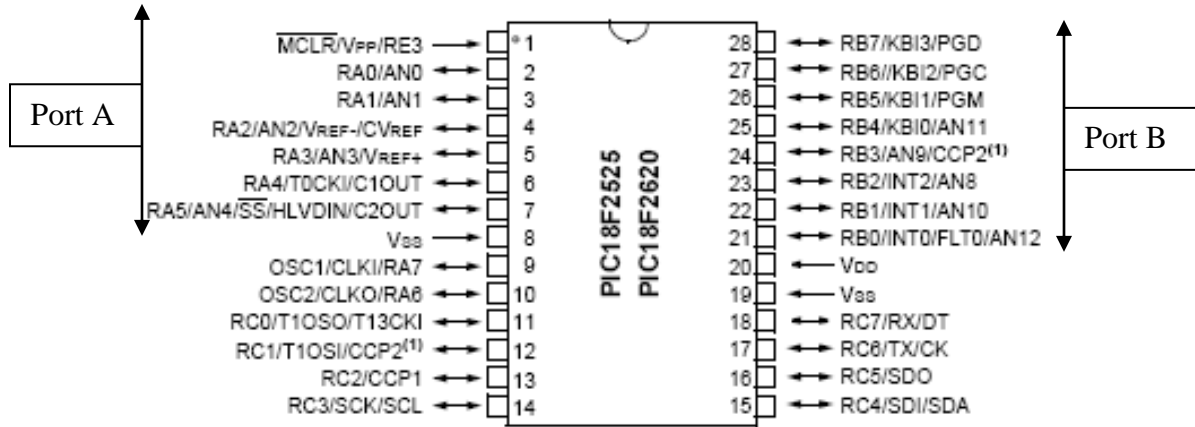


Figure 3: Pin diagram for the 18f2620 used for the payload

Analog to Digital and EEPROM

The microcontroller was used to digitize sensors signals and store the digitized data into its non-volatile memory (EEPROM).

The 18f2620 microcontrollers have a 10-bit or 8-bit ADC integrated into the chip and is accessed through the software. An 8-bit ADC was selected as each data conversion would take up only one byte of address space as opposed to the two bytes for a 10-bit reading. The acquisition time was selected as long as possible as measurements were taken every 1.5 minutes in-flight and as there was no need to make rapid measurements. The conversion was clocked at 1MHz using the internal oscillator with not a lot of precision, but measurements were taken at 0.01Hz and thus the inaccurate high speed clock would not affect time measurement intervals. After each conversion the data was stored into one of the 1024bytes available in the microcontroller's EEPROM. The measurement intervals were timed with a flashing LED and a stopwatch.

Challenges

Due to the unfamiliarity amongst group members with PIC microcontrollers, the programming and operating of the microcontroller had a steep learning curve.

Some of the main challenges that were overcome were becoming familiar with microcontroller software architecture, programming a PIC in C and comprehending the microcontroller datasheet. The C language is not a commonly used language for PIC microcontrollers (Assembler is more commonly used) and thus the group had a lot of difficulty finding example code for the particular PIC device. This frustration was compounded by the compiler (MPLAB C18) compiling code which was actually

incorrect, i.e. the code would compile without error warnings but the microcontroller would not run it. Several weeks were wasted trying to get the microcontroller running code that it could not understand. Table 2 shows an example of incorrect code that giving the group problems.

Table 2: An example of code that would compile and but not run on the microcontroller.

Comment	Code for access data EEPROM memory
Compiled, did not work on PIC	EECON1<7>=0;
Compiled, worked on PIC	EECON1bits.EEPGD=0;

Some other difficulties included timing code for interval readings or camera shutter control. The group was unable to use the compiler’s simulator to give accurate timing of code. The crude solution resorted to looping a flashing LED and timing intervals manual with a stopwatch.

Camera system

The initial design for the camera involved stripping all the unnecessary components (casing, flash, batteries) from an older 3 MegaPixel Gateway digital camera which was donated to the project. The screen was modified to be turned on and off to save power. All the electronics were to be placed in the insulated capsule while the 26 and 20 pin 0.5mm ribbon cables were to be extended so that the lens could sit outside on a servo motor to take pictures at various inclinations. Wires were run from the PIC to the firing button contacts to activate the camera electronically. Unfortunately reliable contact between the ribbon cables and ribbon cable extensions was not achieved despite multiple soldering efforts and a mechanical clamping system. At this point the initial plan was abandoned. All the previous effort was not entirely in vain, the experience gained was used to quickly modify the newer camera.

A 7MP Casio Z75 was ordered to replace the old 3MP camera (still operational). Due to errors by the vendor this camera was not received on time and a 6MP Kodak was used in exchange for the Casio. The camera was connected to the capsule’s 5V power supply and mounted on an aluminum swing actuated by a servo motor to allow the camera to look anywhere between ± 90 degrees from the horizontal. Wires were connected to the firing button. Two outputs from the PIC opened the gates to two n channel transistors which would first auto-focus the camera and then fire it. The setup is given in Figure 4. The PIC was used to provide the pulses necessary to move the servo motor. Although these were properly tuned at one point, the timing of the PIC changed upon modifying the program and the servo motor became unreliable and was not used in the final launch. The camera was set at roughly -30 degrees from the horizontal. The stripped 3MP camera weighed in at 100g, the new camera was approximately 160g.

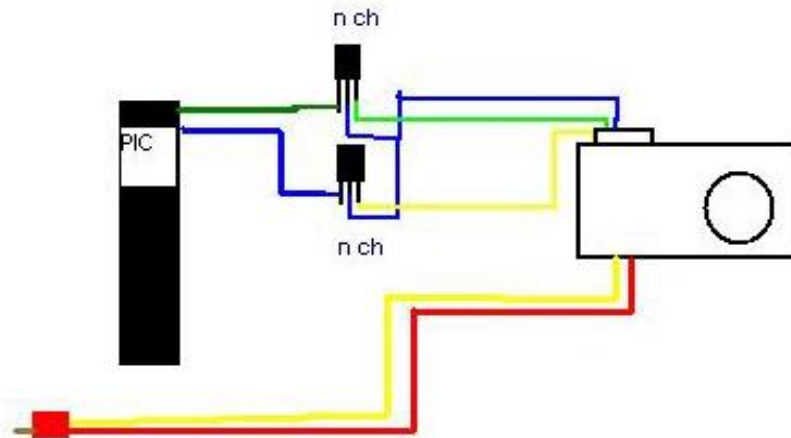


Figure 4: The electronic design for the camera system used

This system worked reliably, the PIC fired the camera every 17 seconds. 627 Pictures were recovered from the flight. 823mb of memory was used from a total of 1gb available. It is has been concluded that the camera ceased operation at an altitude of roughly 28km due to low temperatures and lack of insulation.

Sensors

Purpose

The payload was equipped with sensors to investigate the altitude dependency of atmospheric temperature and pressure. These readings would also provide us with variable data corresponding to the payload's altitude throughout its flight.

The sensors were designed to withstand maximum temperatures of -55°C by using military grade operational amplifiers (Texas Instruments TL074M Quadamps). All measurement circuitry used metal film resistor which have small temperature dependencies. The circuitry was made temperature independent by employing the use of resistor ratios. It could be assumed that any change in resistance due to temperature effects would be identical for each single resistor, and thus the resistor ratios would not change.

Temperature Sensor

The balloon was equipped with a temperature sensor to track changes in temperature from the launch to landing. This data was hoped to provide the group with further altitude dependant data and some interesting temperature curves, and an indication of layers in the atmosphere.

The balloon's ceiling height allowed it to cross the tropopause, the boundary between the troposphere and stratosphere as seen in Figure 5. The tropopause is defined by the lowest temperature drop in the stratosphere, at around $-50\text{ }^{\circ}\text{C}$. The temperature remains constant from between $\sim 10\text{ km}$ to $\sim 20\text{ km}$.

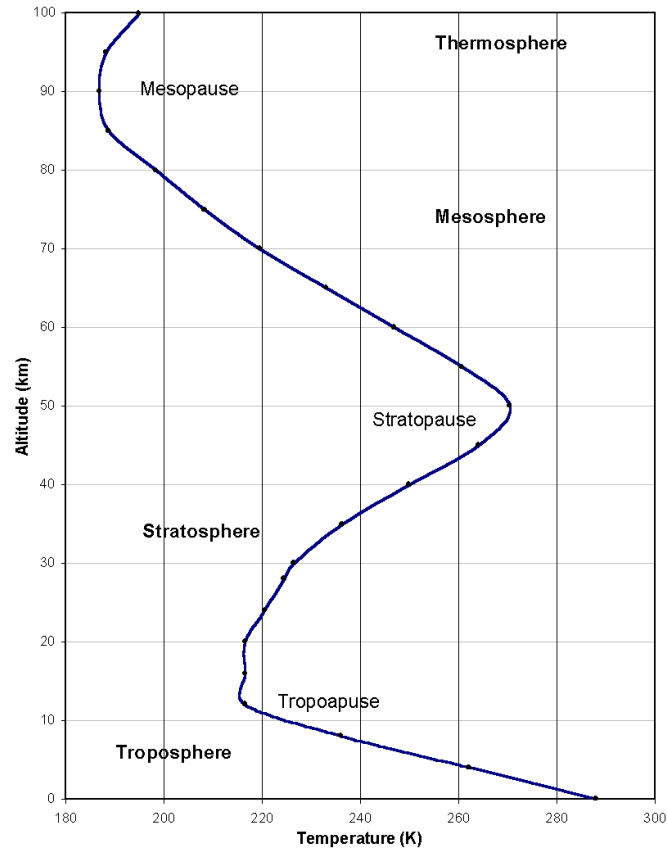


Figure 5: A plot of temperature versus altitude (UofT)

A thermistor was used as the temperature transducer as they are small, cheap and rugged. The low resistance thermistor was selected with a negative resistance coefficient; it increases in resistance with a decreasing temperature. This was desirable as the extreme temperature's concerning the balloon flight were lower than sea-level temperatures where a positive resistant coefficient thermistor may short at low temperatures.

A constant current of 0.1 mA was sent through a $1\text{ k}\Omega$ resistor and the voltage change due to temperature change was measured across the thermistor as shown in Figure 6. The amplification of the signal was necessary in order to increase the apparent sensitivity of the transducers and offset the transducer signal to operate within a desirable temperature window. The operational amplifier also buffered the thermistor from the microcontroller. The current source circuit and offset voltage circuit can be viewed in Appendix A and Appendix B respectively.

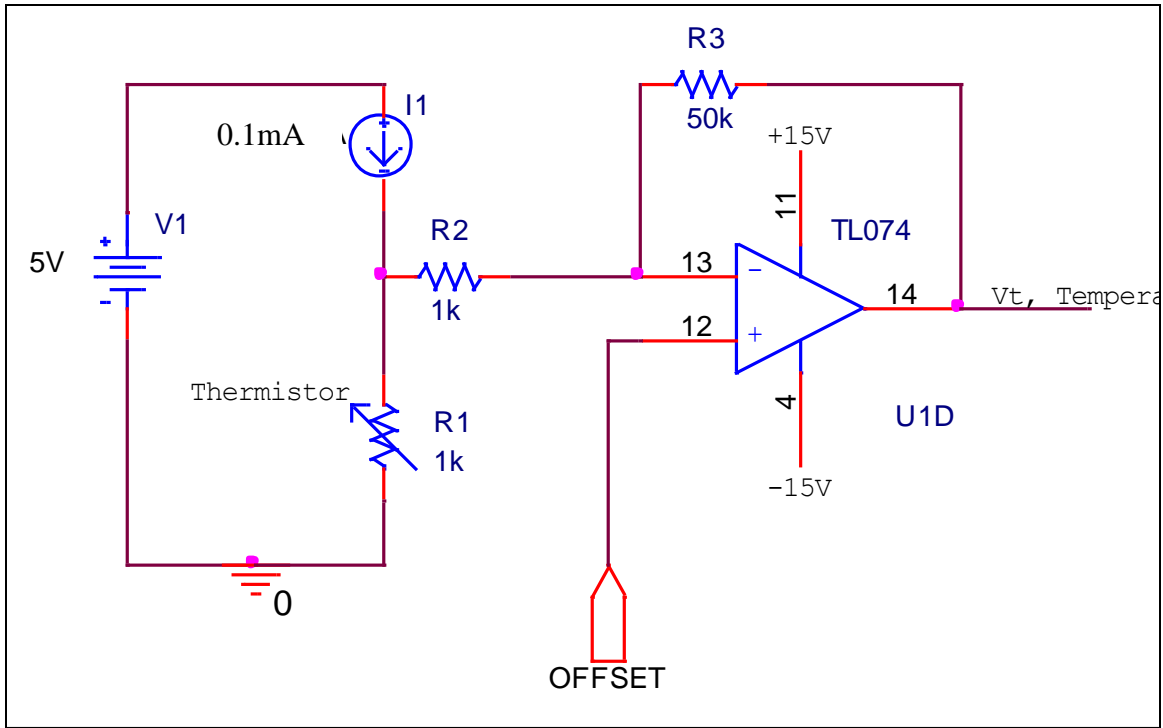


Figure 6: Simplified Diagram of Current Source, Thermistor and Op-Amp with Offset

A calibration curve of the sensor circuitry was made by placing the thermistor at the head of a thermocouple probe. The thermistor and thermocouple were placed at varying heights in a Dewar flask of liquid nitrogen, which gave temperatures from 0 °C to -65 °C and the resulting curve can be seen in Figure 7. The calibration data contained random error, as the probe was held by hand above the liquid nitrogen and any small shake or movement from the person holding the probe, could vary the temperature by a few degrees Celsius. The main purpose of the calibration was to find the resistance of the thermistor at -60 °C; the assumed limited minima for the balloon flight.

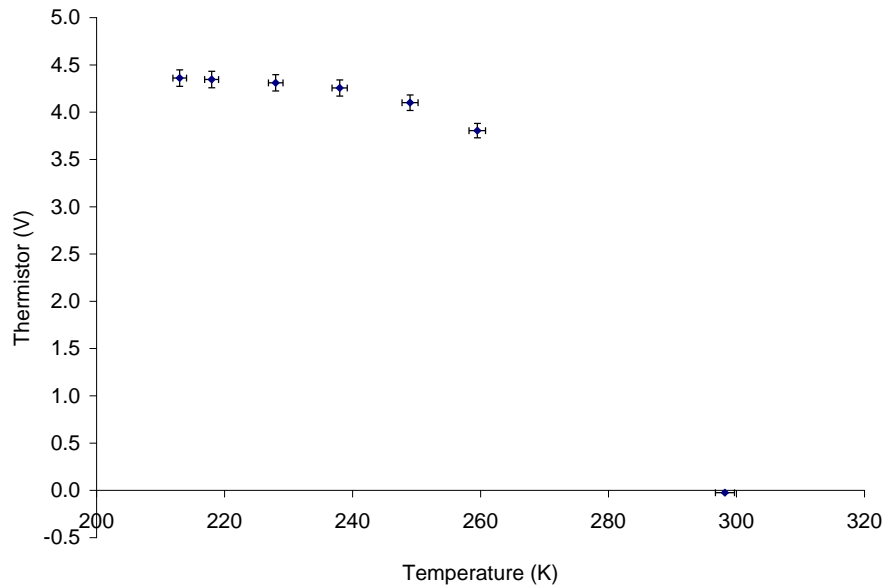


Figure 7: Calibration Curve of temperature sensor output (V) versus thermocouple readings

The sensor ranged in a resolution of 3 °C at -65 °C and 0.5 °C at 0 °C.

Pressure Sensor

Recording the pressure during flight it would give a better indication of altitude than solely measuring temperature (disregarding GPS measurements). The pressure-altitude relationship can be seen in Figure 8, and giving an exponential decay with increasing altitude.

A Motorola MPX100 piezoresistive absolute pressure transducer was used in the sensor. It has an operating pressure of -40 °C to 125 °C and the temperature compensation of readings can be found in the MPX100 datasheet. The transducer was powered by the 5V supply and would give 0.6mV/kPa and is represented in Figure 9. The ADC was only capable of a 20mV resolution and thus the transducer was amplified by a gain of 61. The potential across the two outputs was fed into an instrumentation amplifier as seen in Figure 9 where $V_s=5V$. The “classic three op-amp” instrumentation amplifier was selected for amplifying the transducer. Instrumentation amplifiers have good S/N characteristics and the gain can be easily increased or decreased by changing only one resistor (Kitchin *et al*).

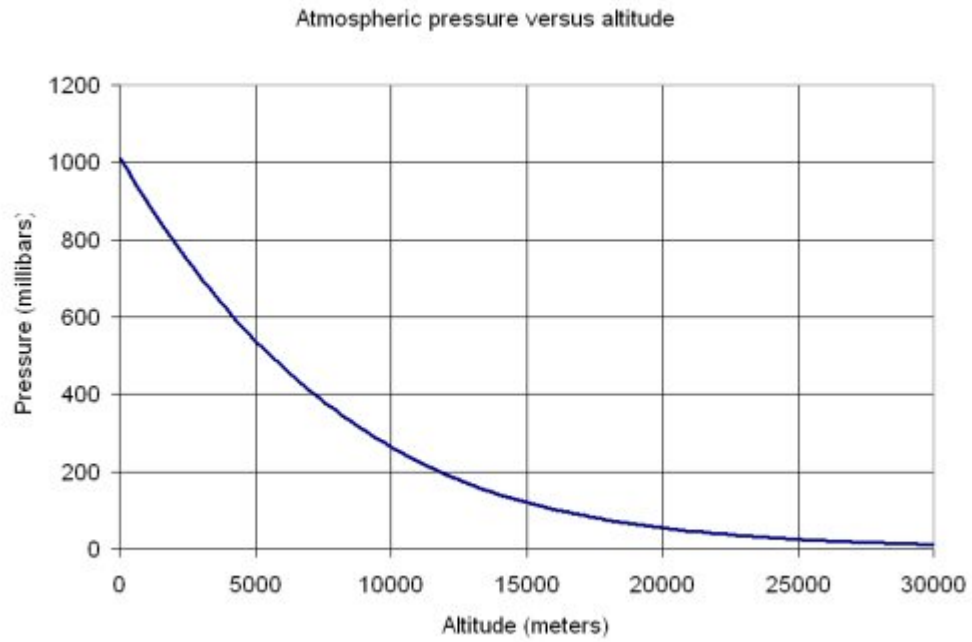


Figure 8: Atmospheric pressure versus altitude

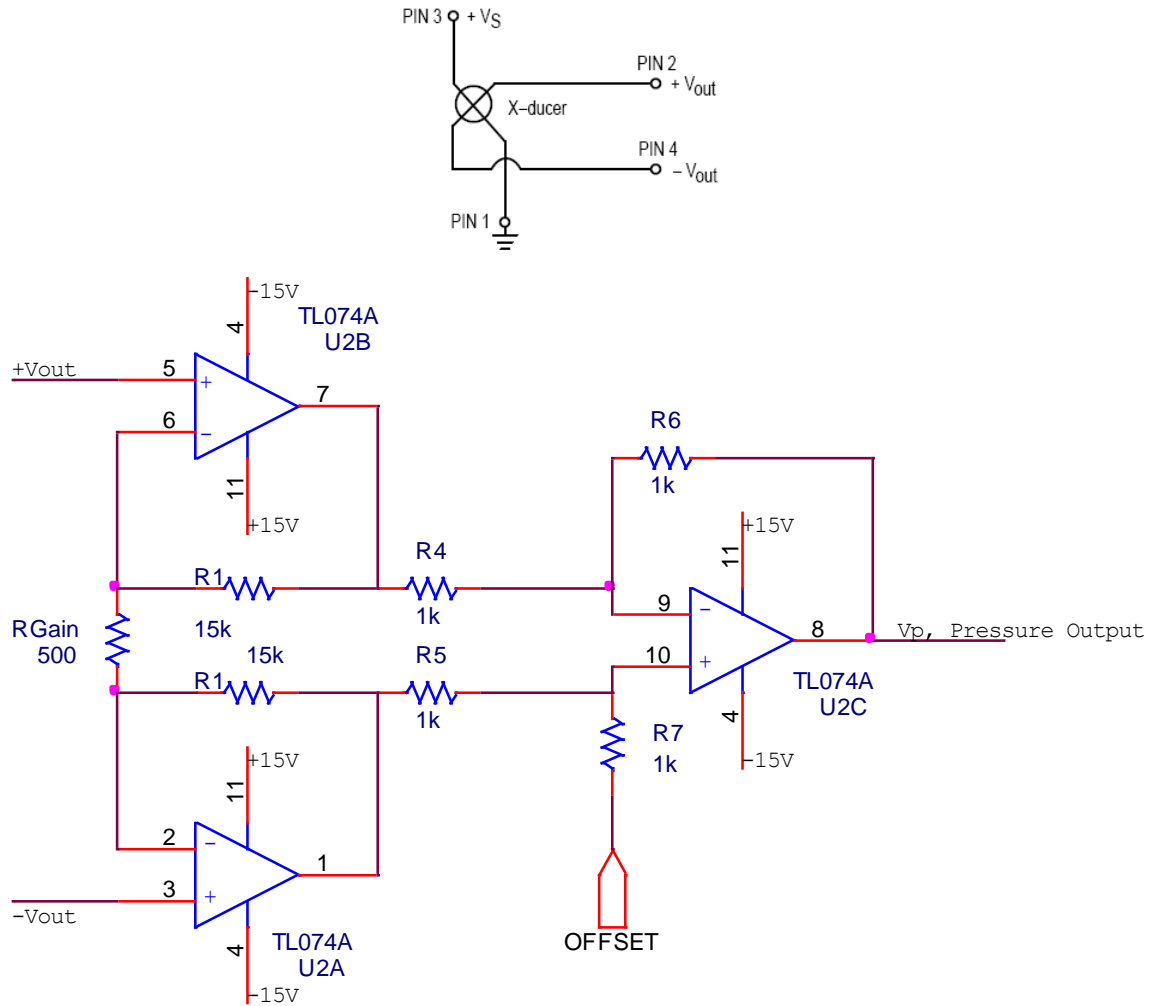


Figure 9: Instrumentation amplifier for the MPX100 Motorola pressure transducer

The gain is varied by changing the value of R_{gain} . The pressure sensors were offset to record readings above 10km and to give an accuracy of 500 Pa. At an altitude of 32km the static pressure is 870 ± 10 Pa; therefore the resolution would be sufficient up to that altitude. The pressure sensor was tested at 120 Pa using a vacuum chamber and the datasheet calibration curve was confirmed (see Figure 10).

$$G_p = \frac{V_p}{V_{-out} - V_{+out}} = \left(1 + \frac{30k\Omega}{R_{gain}} \right) \quad (1)$$

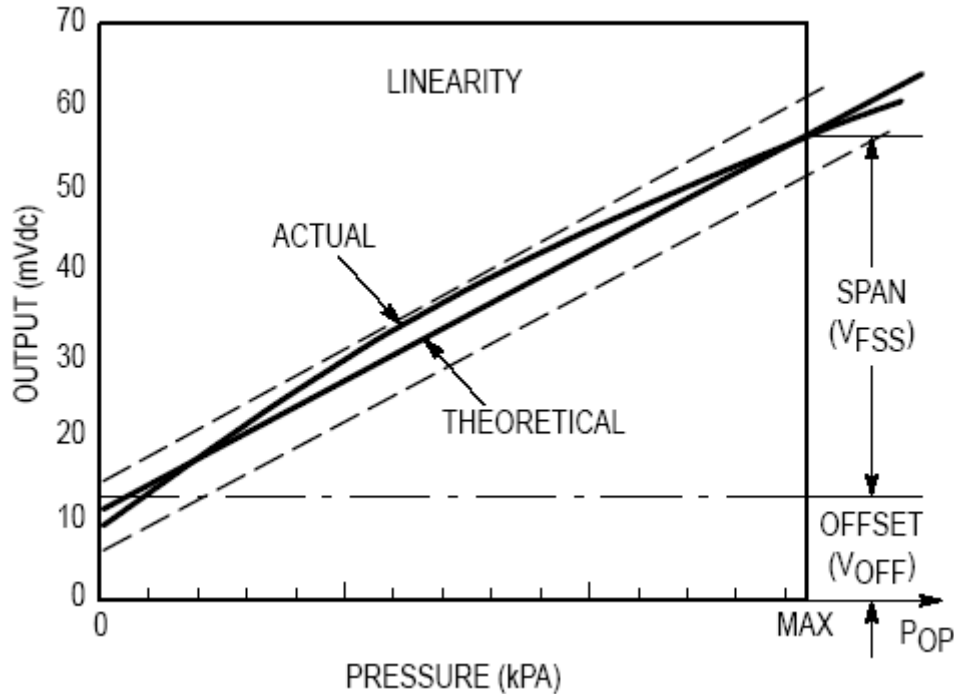


Figure 10: Unamplified MPX100 transducer output taken from the Motorola MPX100 datasheet

Sensors During Flight

On the day of launch the $\pm 15\text{V}$ supply stopped working. This ultimately prevented the payload from reading the sensors as all the op-amps were unpowered. The supply stopped working for unknown reasons, as the sensors had worked that morning of the launch day in the Queen's University Physics labs. The sensors were the only component of the electronics powered by the $\pm 15\text{V}$ supply. The current draws of the sensor were calculated to be below the 33 mA maximum.

There had been some difficulty with the $\pm 15\text{V}$ supplies in the past. Two had been destroyed in the previous weeks to the launch. One incident involved accidentally shorting the supply inputs and the other incident may have been due to a sensor offset voltage divider drawing too much current. At the launch site some untested soldering was carried out on the instrumentation circuit board, possibly shorting something along the $\pm 15\text{V}$ supply.

The $\pm 15\text{V}$ supply problem could have been avoided if a spare supply was brought to the launch site, knowing that there had been previous difficulties with this particular supply. Testing for shorts using an ohmmeter, before powering up the circuitry, has prevented ruining electronic devices in the past and should have been carried out on the launch day.

In future by being aware of the current drawn of devices with respect to their supply and testing for shorts, whenever powering a circuit, could prevent destroying critical components of a circuit.

Cosmic Ray Detector

Introduction

Large quantities of high energy cosmic rays from the sun and other extraterrestrial sources impinge on Earth constantly. These particles are highly attenuated by the atmosphere, where cosmic ray activity is negligible near the surface, which is essential to the existence of human civilization. However, high up in the atmosphere, cosmic ray activity is not negligible and can become quite significant at the design altitude of the balloon.

Near the surface, there are many sources of background radiation, but high up in the atmosphere nearly all radiation is from cosmic ray activity. A system to measure the cosmic ray activity as a function of time was designed, constructed, tested, and fully automated before insertion into the payload capsule. By correlating the activity-time data with pressure-time measurements, cosmic ray activity as a function of altitude could be obtained. Following the exponential decay law, we expected an exponential increase of the activity with height above the surface.

As with the rest of the instrumentation of the balloon, the design constraints of the system were:

- Powered by a 8V battery supply
- As light as possible – no individual weight limitation was specified
- Fully automated

An additional constraint which arose due to a change in direction of the pre-amplification method, limited electronic components, and a lack of time to order additional parts was that the entire cosmic ray detection system had to use a separate common circuit point which was +24V higher than the ground of the rest of the payload instrumentation. This was achieved by carefully separating the circuitry and ground-case of the system from all other systems in the payload.

Detector

The detector used was a reverse biased Si diode semiconductor detector. It was an Ortec BU-CAM-600 designed to measure alpha particles. The detector area was 600 mm². This detector was the most suitable detector for our purposes that was available and could be borrowed. Although the majority of cosmic ray activity in the atmosphere is protons,

about 9% exists as alpha particles (Yao). Due to the small detector area, detector efficiency, and the detector being designed for alpha particles, we were unsure of the actual count rates, if any, that we would obtain. Instead of choosing our counting time based on our expected count rates, we chose the counting time based on the amount of memory we had and the expected flight time.

Power Supply

The pre-amp required a power supply of +24V and -24V at 1.8 mA. According to its data sheet, the detector required a reverse bias between +15V and +24V. Although the detector had been tested to operate at lower bias voltages, +24 V was used due to its availability from powering the pre-amp. We did not have the components required to supply -24V relative to the payload ground, and thus a separate common point had to be used. The required voltages were achieved from a UC2577TD-ADJ switching regulator as shown in Figure 11.

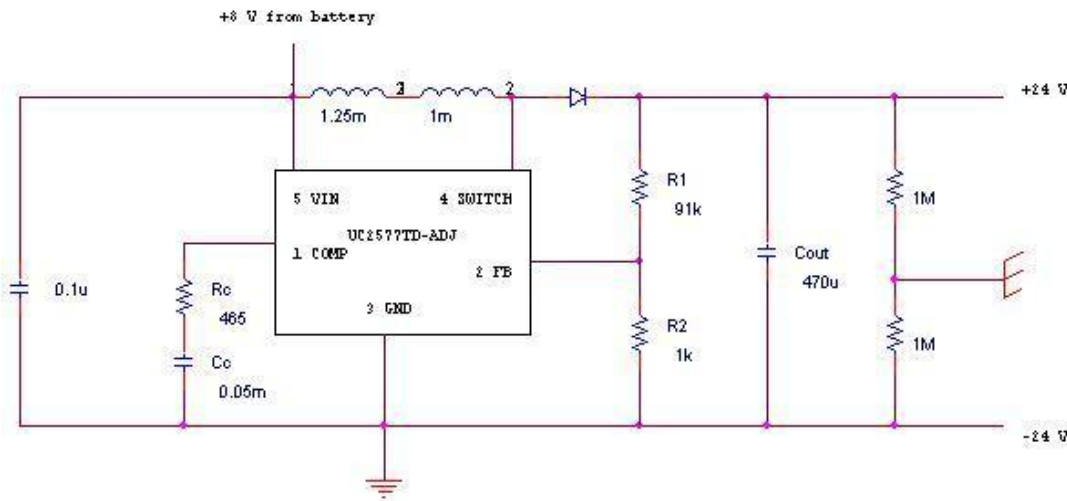


Figure 41: Circuit for providing +24V and -24V.

The 8V input from the battery was stepped up to +48V and fed into a voltage divider to supply +24V and -24V. The circuit was designed and built based on the regulator data sheets and testing. The regulator was designed to handle large currents on the order of amps, and much extrapolation of the data sheets and testing had to be done to provide the required voltages at low current in order to save power. A detailed design methodology and calculations of the power circuit is provided in Appendix C.

Signal Amplification

A block diagram of the system setup is shown in Figure 12.

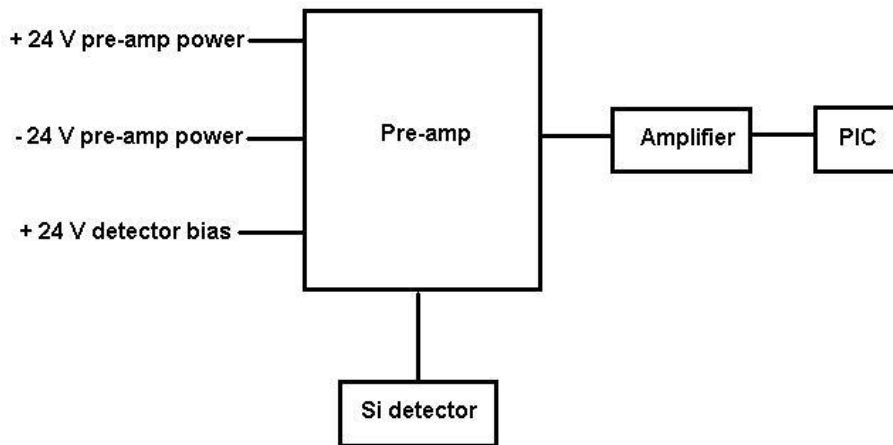


Figure 15: Block diagram of cosmic ray detection system.

The pre-amp used was an Ortec model 118. The metal casing was removed and replaced with a cardboard case wrapped in aluminum foil in order to reduce weight. The amplifier was a LM111 comparator which stepped from high to low on a count. The amplification circuit is shown in Figure 13.

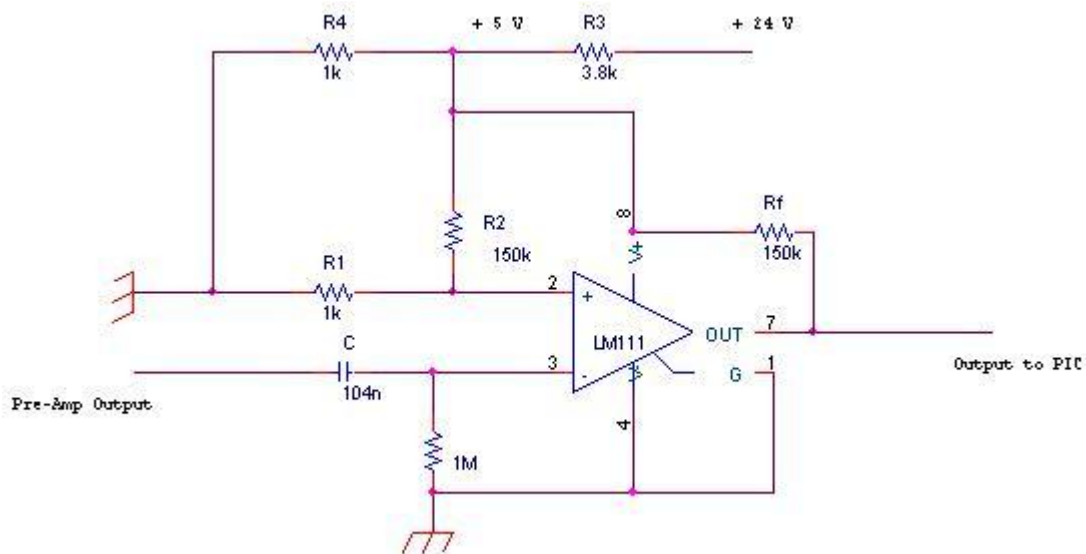


Figure 16: Comparator circuit used in amplification of detector signal.

The reference voltage provided from a voltage divider was 30 mV, and was based on the pulse heights measured from a ^{241}Am alpha source used in tests. A capacitor was used to provide AC coupling to the comparator. The output was sent to a PIC for data collection.

In order to match the digital input to the PIC, a 5V supply was required for the comparator. This was provided from a voltage divider using the +24V available from the voltage regulator.

Testing

Rigorous tests of the detector, pre-amp, and comparator were done with an oscilloscope and an alpha source. After all components were found to work in tandem, all the pieces were soldered together onto a board and tested further.

In writing the PIC program, consideration of the PIC processing speed was taken into account. The PIC operates at 8 MHz, much faster than any count rate we expected. However, we had to ensure that the fast processing speed did not record multiple counts for a single hit on the detector. This was done by introducing a 50 μ s dead time after each count, which was roughly twice the average pulse time as seen on the oscilloscope. Since we expected a very low count rate, this dead time was not expected to cause any counts to be missed. An individual PIC was used for the entire cosmic ray detection system due to its availability, our lack of knowledge in multi-tasking PICs, and the need to have the system at a different common than the rest of the payload. The PIC recorded the total number of counts in 3 minute intervals.

Tracking System

Tracking using radio communication was a subject which no member of the group had any working knowledge of. It became clear that in order to transmit position data a GPS along with a terminal node controller and a transmitter would be needed. Receiving the data could be accomplished with a receiver attached to a TNC on the ground. Setting up a reliable transmitting and receiving system which would meet the power and weight requirements with limited knowledge proved to be challenging. Advice was sought from a local pilot, Barry Smith, whose hobby involved tracking his aircraft using amateur radio frequencies. Barry Smith pointed us in the direction of www.byonics.com, a small company specializing in radio frequency tracking equipment. Barry also pointed out that making any sort of system ourselves to transmit data (telemetry) could be much more sophisticated than we thought. Packets used for radio communication must be appropriately “shaped” to ensure proper reception. For Barry the TinyTrak 3, a radio modem had proven to be reliable; this was hooked up to a standard transceiver and placed in a box. Eventually it was decided that the MicroTrak 8000F/A would be the ideal candidate for tracking the balloon. It combined a TinyTrak3 modem with a transmitter in a light weight and reliable package. A simple serial connection to a GPS would allow the MicroTrak to periodically transmit its coordinates. This product did not allow telemetry but the convenience and low cost (180\$) outweighed the cost of not using telemetry.

A Garmin 18 OEM GPS was procured from the Physics department and modified to a standard serial connection. GPS do not output any position data above 20km high. This is

to prevent their use in terrorist missiles. Throughout the mission the GPS functioned as expected.

In order to procure support and further advice a presentation was made to the Kingston Amateur Radio Club on February 6th. The club agreed to buy and lend us the MicroTrak 8000F/A on the condition that it be returned to them if the balloon was successfully recovered. Since an official HAM radio license is required to transmit on these frequencies the club lent us one of their call signs: VE3KAR-11. They also pointed us towards a report on a similar project which had recently been launched from Perth Ontario.

Once the MicroTrak arrived it was set to transmit at 8W on 144.390MHz. After the GPS locked onto satellites, the position data was immediately picked up by local “repeater” stations and uploaded to the internet on the Automatic Position Reporting System (APRS). www.aprs.fi or www.findu.com. These sites would place a marker (in our case a balloon) onto Google Maps in the last known location of the balloon. They would also store the raw packet information for further analysis. The MicroTrak transmits a short string of characters called the Beacon which is displayed on the tracking sites. This beacon can be changed in the setup while the device is serially connected to a PC. It was initially set to “QUEENS BALLOON” and it was thought that this could be changed periodically by a PIC trying to emulate serial communication from a PC to provide telemetry. Given our difficulty with the PICs this idea was quickly abandoned.

It is important to note that 8W is a considerable amount of RF power. In the experience of other tracking hobbyists, powers on the order of 300mW can achieve reliable communication through the atmosphere. 8W was selected based on the available power from the batteries and based on the need to ensure reception once the balloon has landed in its final location. A quarter wave whip monopole antenna was borrowed from the KARC. During the flight it was oriented vertically. This was done to ensure a strong radiation field upon landing, assuming the balloon landed upright or got stuck in a tree as was expected.

In order to completely test our tracking abilities, particularly the ability to monitor altitude, the partially completed capsule along with some members of the group were taken up in one of OFF’s (Kingston’s flight school) Cessnas.. During this “field trip” Barry also demonstrated and helped us set up the necessary software to track the balloon from a laptop connected to a receiver. The test flight trajectory is shown in Figure 14. The flight demonstrated the tracking unit’s abilities and revealed that the frequency of transmission need to be increased from once every 2 minutes to once every 21 seconds in order to ensure recovery of the payload.

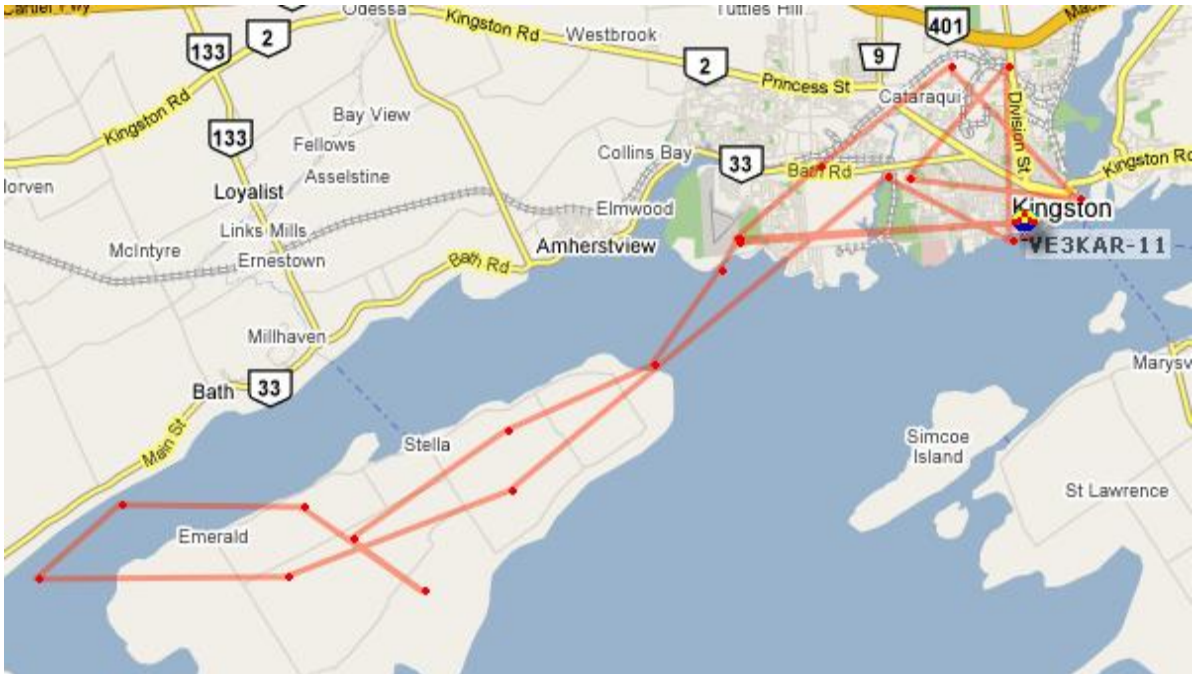


Figure 14: Flight path of the test flight. Note the large gaps between transmission which occurred every 2 minutes.

In order to eliminate complicated external hardware (a TNC) while remotely tracking the balloon a receiver was directly connected to the sound card of a laptop. With the use of a program called AGPWE, the radio packets received from the balloon could be interpreted by the computer. AGWPE was used in unison with another program; UIView32. UIview is available to HAM users. The program would read the packets from AGWPE and place a marker on saved maps in the current location of the balloon. The small antenna on the receiver allowed only for a limited range. This system worked semi-reliably until the balloon passed above 20km. Once it did, packets could be received but not interpreted as expected based on the GPS operation.

Throughout the process of this project, new tracking technology became available. The TinyTrack4 was released. The company claimed it could do telemetry, however since this was not offered with a compact transmitter like the TinyTrak3 (in the MicroTrak) and since it was still an infant product it was not used. It was also unclear as to how telemetry could be received and interpreted based on our knowledge of the available software.

The robust tracking system led to complete tracking of the payload throughout the mission and to a successful recovery. The network of radio “repeaters” close to the flight path assisted in tracking the balloon while the small receiver was out of range.

Cut Down Timer

The use of a cut down timer was recommended in many reports on previous high altitude balloon projects. The connection between the parachute and the balloon would be cut after a certain amount of time releasing the payload into freefall. This is appropriate for the scenario where the balloon does not pop at high altitude and continues to drift. The use of a cut-down timer would have been extremely beneficial to the recovery of our capsule. A design was attempted where a high current was sent through a ¼ Watt 1 Ohm resistor, heating the resistor and melting a nylon rope. This system was demonstrated in the lab 3 times with a wall power source before it was pursued. Monostable 555 timing circuits were experimented with however it was found that too large a capacitor would be needed to achieve the desired period and they could easily be falsely triggered.

The final design involved connecting the buzzer outputs of a kitchen timer to the trigger of a monostable 55 timing circuit. After the pre-set timer triggered the timing circuit, a 5 second 5V pulse would be applied to an N-Channel MOSFET capable of sinking the 4-5 Amps required to heat the resistor to cut the balloon down. See Figure 15 for the diagram. Again the timing circuit proved far too volatile, it could be set off accidentally by moving the electronics around. This could be because of poor connections due to the use of a protoboard and the cut down timer was not used. Cutting down the balloon at a small altitude due to say a current being induced in the trigger from the high RF power could have been disastrous.

The designed 555 timing circuit is shown in Figure 16. The timer which supplied a voltage of 0.1V was connected to a p channel transistor. This was connected to the gate of a larger N-channel MOSFET. The timer supplied a 1s pulse with a period of 2s. With the appropriate current 1s was just enough to heat the resistor and cut the rope. The final test of this important circuit failed prior to launch and thus it was not included. It is thought that some resistors simply opened the circuit before they could adequately heat up. The total resistance of the wires and the resistor in the circuit was measured at 2.3 Ohms. If the MOSFET was opened and a potential of 8V was applied there would be a current of 3.48A would pass through the 1.8Ohm resistor, dissipating 11W.

If this circuit was included and worked properly the balloon would have been cut down dangerously close to the St. Lawrence however it would have not been capable of taking off again the next day to travel further South (see flight path analysis).

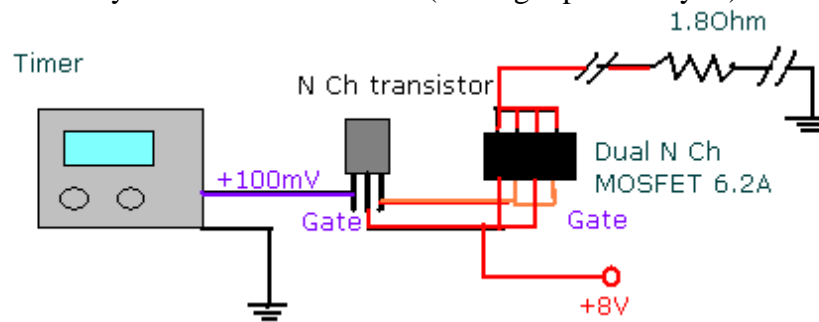


Figure 15 - Cut down circuit planned for use.

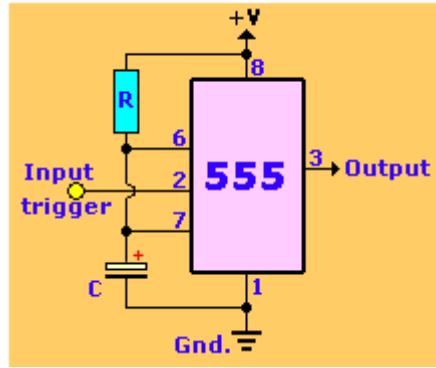


Figure 16 - 555 timing circuit. The trigger would have been placed at the output of the N Ch transistor and the output connected to the MOSFET gates.

Photos and Analysis

The camera used to capture images during flight was a Kodak EasyShare C643 6.1 Mega Pixel digital camera. The images captured were used as a means of calculating an approximation to the altitude obtained by the balloon during flight. The relevant camera specifications are given in Table 3

Table 3 - Kodak EasyShare C643 digital camera specifications [Kodak EasyShare].

CCD	1/2.5 in. CCD, 4:3 aspect ratio
Output image size	6.1 MP: 2848 x 2134 pixels
Lens	Aperture: maximum - f/2.7; minimum - f/8.5 36 mm - 108 mm (35 mm equivalent)
Focus system	10 m (32.8 ft.)-infinity @ Landscape

The camera was set to Landscape mode which focuses at 10m (hyperfocal distance) to infinity. When the camera is focused at the hyperfocal distance, all objects at distances from half of the hyperfocal distance out to infinity will be acceptably sharp. The hyperfocal distance can be calculated using the following formula:

$$H = \frac{f_{35}^2}{ND} \quad (2)$$

Where H is the hyperfocal distance, f_{35} is the 35mm equivalent focal length in millimeters, N is the f-number, and D is circle of confusion limit. The circle of confusion used in 35mm photography is 0.03mm. Landscape mode is basically a large depth of field mode. Depth of field is the amount of the image before and beyond the focus point that will be in focus. Landscape is programmed to give the smallest aperture (largest f-stop) possible in order to ensure a large depth of field. That is, the f-number used in landscape mode by the camera was 8.5. Therefore, the 35mm equivalent focal length was found to be 50.5mm.

The 35mm equivalent focal length refers to the focal length of a 35mm film camera required to provide the same field of view (FOV) as the digital camera. Just to be clear, 35mm is not the focal length of the film camera but rather the overall width of the film as shown in Figure 17.

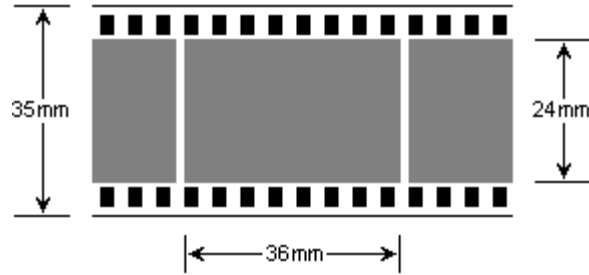


Figure 17 - Film dimensions [Panorama Factory].

Therefore, a schematic diagram for a 35mm film camera with a focal length of 72mm is shown in Figure 18.

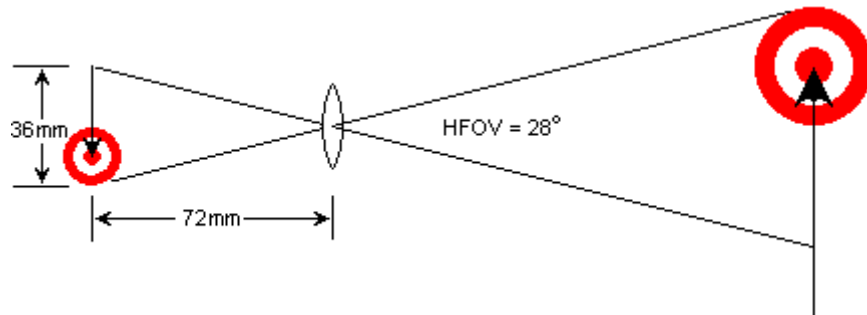


Figure Error! No text of specified style in document.18 - Schematic diagram of a possible 35mm camera focal length [Panorama Factory].

Now, since the aspect ratio of film cameras (3:2) differs from that of the digital camera used (4:3) the 35mm equivalent focal length must be converted into a true focal length, f , based upon horizontal field of view. The relationship between f_{35} and f is given in Equation 2.

$$f_{35} = 36.0 \frac{f}{w} \quad (3)$$

Where w is the width of the charge-coupled device (CCD) array in millimeters. Digital camera sensors (in this case a CCD) are often referred to with a 'type' designation using imperial fractions such as 1/1.8" or 2/3" which are larger than the actual sensor diameters. The type designation dates back to a set of standard sizes given to TV camera tubes in the 1950's. The size designation does not define the diagonal of the sensor area but rather the outer diameter of the long glass envelope of the tube. The usable area of this imaging plane was approximately two thirds of the designated size as shown in Figure 19.

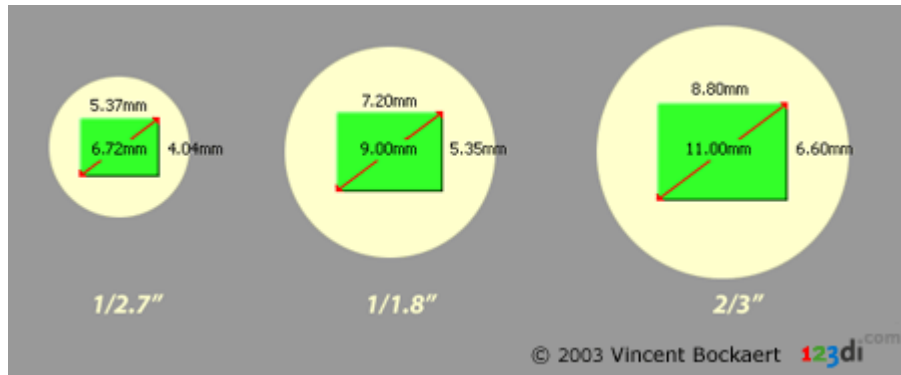


Figure 19 - Sensor sizes [Bockaert].

The digital camera used was of the type 1/2.5" and thus had dimensions of: width 5.760mm, and height 4.290mm. It was assumed that the imaging area was equal to 100% of the sensor array. Therefore, it was found that the true focal length was 8.08mm. The field of view of the digital camera in landscape mode can be calculated using:

$$FOV = 2 \arctan\left(\frac{w}{2 \cdot f}\right) \quad (4)$$

It was found that the FOV was 39.2°.

Now, from the images captured by the digital camera it is possible to approximate altitude that the balloon reached during flight. The images captured were taken with an angle of depression which varied over the course of the flight and was difficult to determine. Therefore, the image analysis will initially assume a completely downward perspective and then apply a correction coefficient dependent upon the magnitude of approximate angle of depression to give altitude measurements.

The real distance of the landscape width is D_r and the actual size of the object is x_r . The FOV of the camera is 2θ .

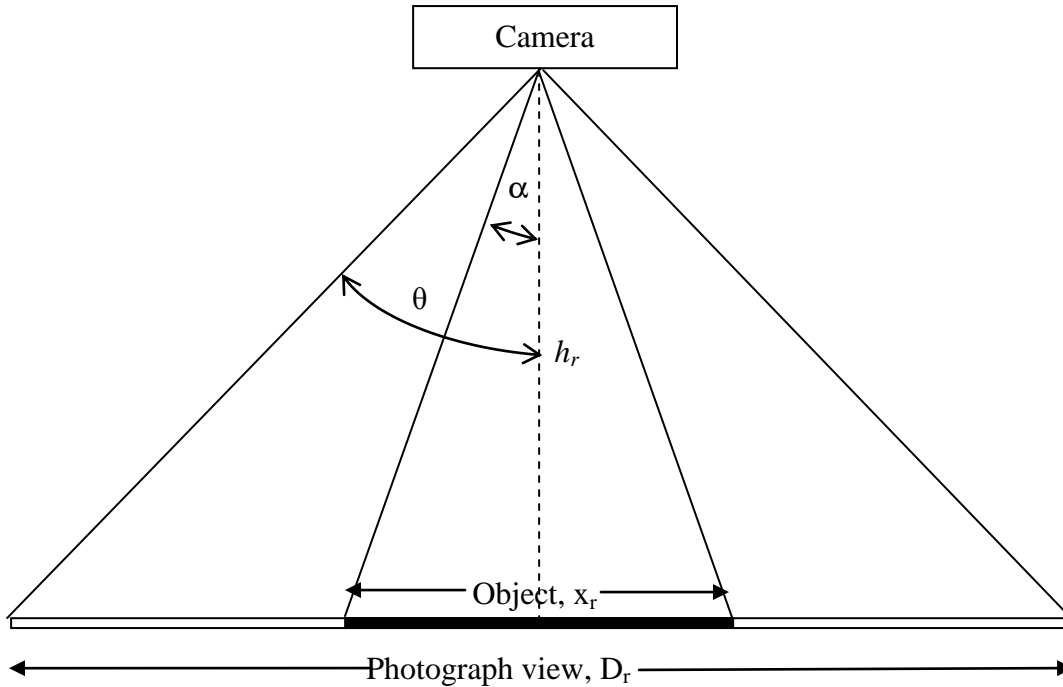


Figure 20 - The field of view of the camera at an altitude of h

The landscape width seen on the photograph D and object size on the photograph x were measured by counting pixels. The trigonometric relationship of the photograph altitude h and the measured photograph dimension and object size are shown by equations (5) and (6).

$$\frac{x}{2h} = \tan \alpha \quad (5)$$

$$\frac{D}{2h} = \tan \theta \quad (6)$$

$$h = \frac{D \cot \theta}{2}$$

A similar relationship is found for the actual object size x_r and actual altitude of the camera h_r in equation (7).

$$\frac{x_r}{2h_r} = \tan \alpha \quad (7)$$

The ratio of object size and altitude are identical for both the photograph and actual dimensions from equation (6) and (7)

$$\frac{x}{2h} = \frac{x_r}{2h_r} \quad (8)$$

$$h_r = \frac{x_r}{x} h$$

In substituting equation (6) into equation (8) the actual altitude of the camera is found to be.

$$h_r = \frac{x_r D \cot \theta}{2x} \quad (9)$$

Therefore, the altitude can be found by knowing the cameras angle of view θ , object size on photograph x , landscape distance on photograph D and the actual size of the object x_r (using Google Earth). It would be possible to calculate the altitude at which each photo was taken if terrain captured in the images were easily identifiable. This was a difficult task since all the images were taken in remote parts of Ontario. However, at approximately maximum flight altitude the balloon captures a recognizable land mass – Hill Island. Using the appropriate equation and measurements from Google Earth it was found that the altitude reached in this photograph shown in Figure 21 was approximately:

$$h_r = \frac{0.13 \text{ km} \left(\frac{848 \text{ pixels}}{2000 \text{ pixels}} \right) \cot(9.6^\circ)}{2} = 42.6 \text{ km}$$



Figure 21 - Image captured near maximum altitude over Hill Island.

Now, the angle of depression must be considered. An illustration of the affect of an angle of depression is shown in Figure 22.

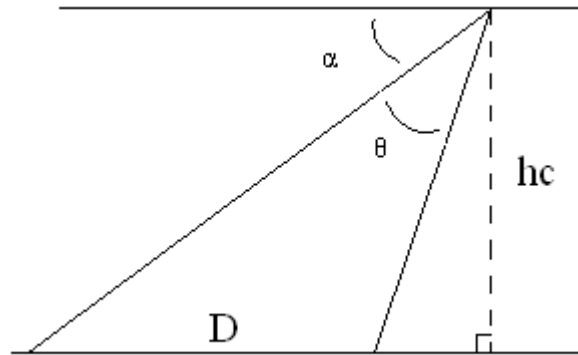


Figure 22 - Schematic used to illustrate the affect of angle of depression.

Using Figure 5 it can simply be shown that:

$$h_c = \frac{2 \cdot h_r \cdot \sin \alpha \sin (\gamma + \theta) \left[\tan \left(\frac{\phi}{2} \right) \right]}{\sin \theta} \quad (10)$$

Where h_c is the corrected altitude, and θ is the angle of depression. Approximating an angle of depression of 50° the corrected altitude was found to be 30.3km which is nearly the theoretical maximum altitude that the balloon should have reached before popping.

Conclusion

The purpose of the balloon was to take photographs and take atmospheric measurements. Systems to measure the pressure, temperature, and cosmic ray activity as a function of altitude were designed and constructed, however, due to weight restrictions and last minute failures, no measurements were taken. The payload was successfully tracked and recovered with all instrumentation still intact. Analysis of the photographs indicated that an altitude of 30.3km was reached which agreed with predicted altitude calculations. Despite several technical setbacks, this project can be looked upon as a reference for future high altitude balloonists as an example of what works well and things that should be avoided or considered in more detail.

References

Kaymont Meteorological Balloons. Retrieved from:

<http://www.kaymont.com/pages/sounding-balloons.cfm>

Kitchin, C. Counts L. *A designer's Guide to Instrumentation Amplifiers 2nd Edition*
Analog Devices Inc. USA 2004

Motorola Semiconductor Technical Data MPX100/D 0 to 100kPa Uncompensated
Silicon Pressure Sensor USA

Yao, W. M., et al. *Particle Data Group review of Cosmic Rays*.
Journal of Physics G 33, 1. 2006.

University of Toronto Temperature-Altitude Plot. Retrieved from:

<http://www.atmosph.physics.utoronto.ca/people/loic/Image1.gif>

Kodak EasyShare C643/C603 Digital Zoom Camera. "User's Guide". Retrieved from:
http://www.kodak.com/global/plugins/acrobat/en/service/manuals/urg00531/C643_C603_GLB_en.pdf

The Panorama Factory. "What is '35mm equivalent focal length?'". Retrieved from:

<http://www.panoramafactory.com/equiv35/equiv35.html>

Bockaert, V. "Sensor Sizes". Retrieved from:

http://www.dpreview.com/learn/?/Glossary/Camera_System/sensor_sizes_01.htm

Appendices

Appendix A: Thermistor Current Source

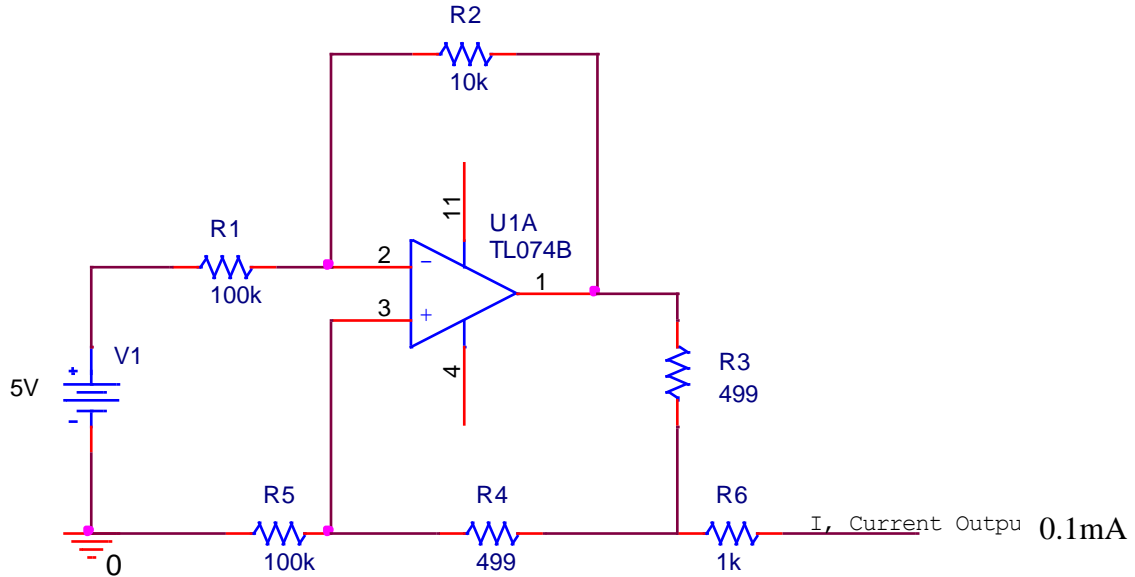


Figure A1: A single op-amp constant current source used for the temperature sensor.

Appendix B: Voltage Offset for Sensors

The pressure sensor offset as seen in Figure B1 could draw maximum current of 3.3 mA as shown in Figure B1.

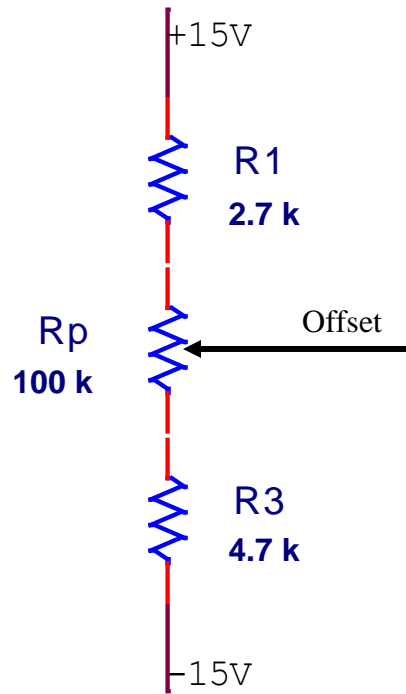


Figure B1: The offset voltage supply used for the pressure sensor instrumentation amplifier

The temperature sensor offset drew a maximum current of 0.3mA, as shown in Figure B2.

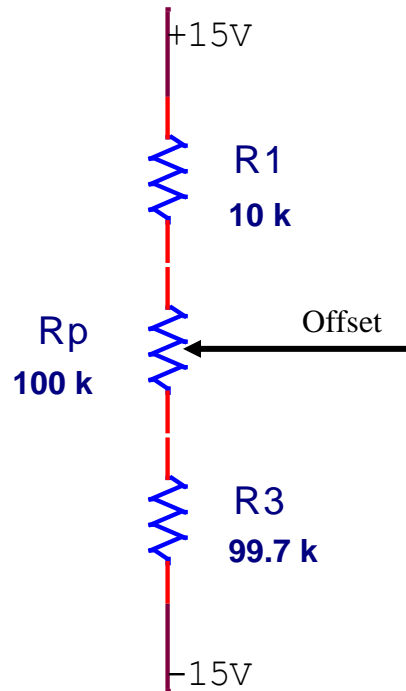


Figure B2: The offset voltage supply used for the temperature sensor amplifier

Appendix C: Design calculations of cosmic ray detector power circuit

The UC2577TD-ADJ is designed to take input voltages between 3V and 40V, and output voltages between 0V and 60V; our required voltages lie within these limits. The regulator is also rated to work down to -65°C temperature.

The circuit is shown in Figure C1. Formulas used in the design calculations were all taken from the data sheet.

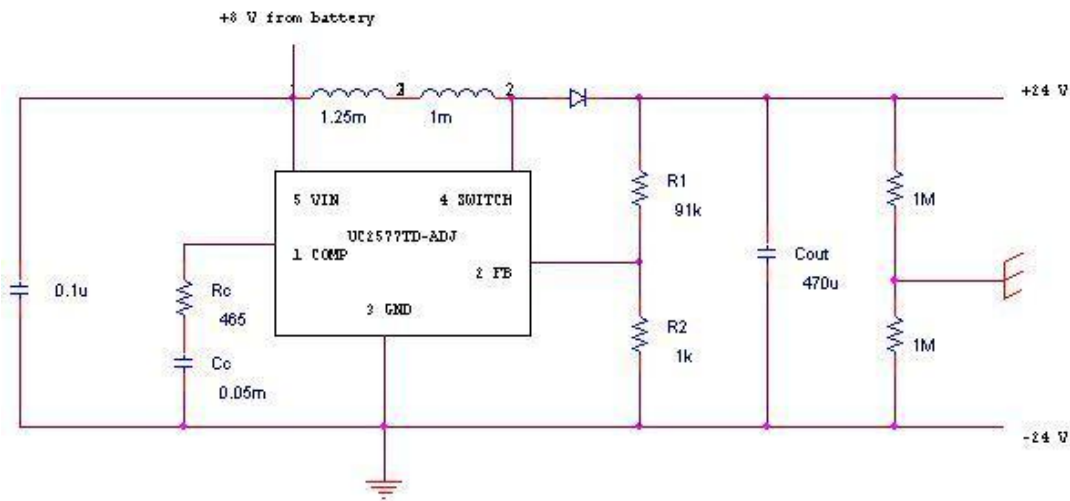


Figure C1: Circuit used to provide +24V and -24V to the pre-amp

The output voltage is controlled by the resistors $R1$ and $R2$. The data sheet states:

$$\frac{R1}{R2} = \frac{V_{out}}{1.23\text{V}} - 1$$

which suggests $R1/R2 = 38$ to produce 48V.

In order to choose the value of the inductance, three parameters were calculated:

The maximum switch duty-cycle, D_{max} ,

$$\begin{aligned} D_{max} &= \frac{V_{out} + V_F - V_{in}}{V_{out} + V_F - 0.6\text{V}} \\ &= \frac{48 + 0.5 - 8}{48 + 0.5 - 0.6} \\ &= 0.846 \end{aligned}$$

where $V_F = 0.5$ for the diode used.

The product of volts and time that charges the inductor, $E \cdot T$,

$$\begin{aligned} E \cdot T &= \frac{D_{\max} (V_{in} - 0.6V) 10^6}{52000\text{Hz}} \\ &= \frac{0.845 (10 - 0.6V) 10^6}{52000\text{Hz}} \\ &= 120\text{V} \cdot \mu\text{s} \end{aligned}$$

The average inductor current,

$$\begin{aligned} I_{ind} &= \frac{1.05 I_{load}}{1 - D_{\max}} \\ &= \frac{1.05 (8\text{mA})}{1 - 0.845} \\ &= 12.2\text{mA} \end{aligned}$$

The data sheet provides a chart that gives an inductor value based on the I_{ind} and $E \cdot T$. However, the lowest inductor current on the chart was 300 mA. An extrapolated inductance value of 2.25 mH was used.

A compensation network consisting of resistor R_C and capacitor C_C which form a simple pole-zero network stabilizes the regulator. The values of R_C and C_C depend on the voltage gain of the regulator, I_{LOAD} , the inductor L , and output capacitance C_{OUT} .

The maximum value of RC was:

$$\begin{aligned} R_C &\leq \frac{7500 I_{Load} V_{out}^2}{V_{in}^2} \\ &\leq \frac{7500 (8 \cdot 10^{-3}) (8)^2}{(10)^2} \\ &\leq 486\Omega \end{aligned}$$

R_C was chosen to be 465 Ω .

The minimum value of C_{OUT} was:

$$\begin{aligned} C_{OUT} &\geq \frac{V_{in} R_C (V_{in} + 0.74 \cdot 10^5 L)}{487800 V_{out}^3} \\ &\geq \frac{(10)(465) + (0.74 \cdot 10^5)(0.00225)}{487800 (8)^3} \\ &\geq 58.6\mu\text{F} \end{aligned}$$

A capacitance of 470 μF was chosen. This large value was chosen as tests of the circuit showed that a larger capacitance provided a more stable output voltage.

The minimum value of C_C was:

$$\begin{aligned}
C_c &\geq \frac{58.5V_{out}^2 C_{OUT}}{R_c^2 V_{in}} \\
&\geq \frac{58.5 \cdot 48^2 \cdot 70 \cdot 10^{-6}}{65^2 \cdot 6} \\
&\geq 36.6\mu\text{F}
\end{aligned}$$

A 50 μF was used for C_c .

A diode that can handle 50V was chosen. A 0.1 μF input capacitor was used to provide decoupling and reduce noise.

Under these calculated values, the regulator was found to regulate the supply voltage at 7V and output 21V. The resistors $R1$ and $R2$ were modified through trial and error until stepping up from 8V to 48V was achieved at a $R1/R2$ value of 91.

Appendix D: Camera Code

```

#include <p18cxxx.h>
#include <delays.h>

#pragma config OSC = INTIO67 /*Internal oscillator */
#pragma config WDT = OFF /* Turns the watchdog timer off */
#pragma config LVP = OFF /* Turns low voltage programming off */
#pragma config DEBUG = OFF /* Compiles without extra debug code */

void delay(unsigned int);

void delay (unsigned int i)
{
    while (--i>0)
    {
        i=i;
    }
}

void main(void) {

    int count;
    int i;
    OSCCONbits.IRCF2=1;
    OSCCONbits.IRCF1=1;
    OSCCONbits.IRCF0=1;
    PORTB = 0;
    TRISB = 0b00111111;

    delay(200);
    for(i=0; i<=10; i++)

```

```

{

    PORTB=0x80; //Yellow and blue - auto-focus
    delay(1000);
    PORTB=0xC0; //Yellow, blue and green - shot

    delay(2000);
    delay(2000);

    PORTB=0;
    delay(100);
}

```

Appendix D: Sensor Code

```

#include <p18cxxx.h>
#include <adc.h>
#include <delays.h>

#pragma config OSC = INTIO67 /*Internal oscillator */
#pragma config WDT = OFF /* Turns the watchdog timer off */
#pragma config LVP = OFF /* Turns low voltage programming off */
#pragma config DEBUG = OFF /* Compiles without extra debug code */

void flashLED(unsigned int);
void eeprom_write(unsigned char, unsigned char, unsigned char);
void atod (unsigned char, unsigned int);
void delay(unsigned int);

void flashLED(unsigned int j)
{
    PORTB=0x80;
    delay(j);
    PORTB=0;
    delay(j);
}

void delay (unsigned int i)
{
    while (--i>0)
    {
        i=i;
    }
}

void atod (unsigned char add, unsigned int channel)

```

```

{
    volatile unsigned current_ad_value;
    char reading;

    //set AN0 as analog and vs and vd as ref
    //ADCON1=0b00001110;// AN0 - A
    ADCON1bits.PCFG3=1;
    ADCON1bits.PCFG2=0;
    ADCON1bits.PCFG1=1;
    ADCON1bits.PCFG0=1;

    ADCON1bits.VCFG1=0;
    ADCON1bits.VCFG0=1;

    if(channel==0)
    {
        ADCON0bits.CHS3=0;
        ADCON0bits.CHS2=0;
        ADCON0bits.CHS1=0;
        ADCON0bits.CHS0=0;
    }

    if(channel==1)
    {
        ADCON0bits.CHS3=0;
        ADCON0bits.CHS2=0;
        ADCON0bits.CHS1=0;
        ADCON0bits.CHS0=1;
    }

    ADCON2bits.ACQT2=1;
    ADCON2bits.ACQT1=1;
    ADCON2bits.ACQT0=1;

    ADCON2bits.ADCS2=1;
    ADCON2bits.ADCS1=1;
    ADCON2bits.ADCS0=1;

    ADCON2bits.ADFM=0; //right justified

    ADCON0bits.ADON=1;
    // Enable interrupts
    PIR1bits.ADIF=0;
    PIE1bits.ADIE=1;
    INTCONbits.GIE = 1;

    delay(200); //wait a little

    // start the ADC conversion
    ADCON0bits.GO = 1;
    while (ADCON0bits.GO==1){}

    current_ad_value = ADRES;
    reading = ADRESH;
}

```

```

    PIR1bits.ADIF=0;

    eeprom_write(0x00, add, reading);

}

void eeprom_write(unsigned char high, unsigned char address, unsigned
char data) //write to EEPROM
{

    //-----

    EEADR=address; //holds from 00h to 3FFh
        EEADRH=high;
    EEDATA=data; //Holds 8-bit data

    //Not sure if these are required-----
//    EECON1bits.EEPGD =0;
        EECON1bits.EEPGD=0; //Access data memory EEPGD
        EECON1bits.CFGS=0; //Access configuration registers  CFGS

    //Writing to EEPROM

        EECON1bits.WREN=1; //Allows a write operation WREN

        INTCONbits.GIE=0; //disables interupts GIE

        EECON2=0x55; //Write Protect "key"
        EECON2=0x0AA; //

        EECON1bits.WR=1; //initiates write/erase cycle (bit 1)  WR

while(EECON1bits.WR == 1) {}

        INTCONbits.GIE=1; //Enables interupts  GIE
        EECON1bits.WREN=0; //WREN disable
}

void main (void)
    {
        char padd;
        char tadd;

        int check;
        int i;
        i=0;

        OSCCON = 0x07; //Sets Internal oscillator to 8
MHz

        TRISA=1; //All porta input
        TRISB=0b01111111; //RB7 output  and RB6 input

```

```
PORTB=0;

padd=0x00;
tadd=0x01;

while(tadd <= 0xff)
{
atod(padd, 0);
atod(tadd, 1);

padd=padd+0x02;
tadd=tadd+0x02;

Delay10KTCYx(60);

}
}
```